

See discussions, stats, and author profiles for this publication at: <https://www.researchgate.net/publication/23273173>

# Thiazin red as a neuropathological tool for the rapid diagnosis of Alzheimer's disease in tissue imprints

Article in *Acta Neuropathologica* · October 2008

DOI: 10.1007/s00401-008-0431-x · Source: PubMed

CITATIONS

35

READS

219

6 authors, including:



José C Luna-Muñoz

Facultad de Estudios Superiores. Cuautitlán. Universidad Nacional Autónoma de ...

86 PUBLICATIONS 1,432 CITATIONS

[SEE PROFILE](#)



Claude Michel Wischik

117 PUBLICATIONS 7,561 CITATIONS

[SEE PROFILE](#)

Some of the authors of this publication are also working on these related projects:



Vision loss in Alzheimer's Disease [View project](#)



Oxidative stress and neurological diseases [View project](#)

# Thiazin red as a neuropathological tool for the rapid diagnosis of Alzheimer's disease in tissue imprints

José Luna-Muñoz · Janneth Peralta-Ramirez ·  
Laura Chávez-Macías · Charles R. Harrington ·  
Claude M. Wischik · Raúl Mena

Received: 6 June 2008 / Revised: 28 August 2008 / Accepted: 29 August 2008 / Published online: 23 September 2008  
© Springer-Verlag 2008

**Abstract** In recent years, we have used a variety of tau immunological markers combined with the dye thiazin red (TR), an accurate marker to differentiate the fibrillar from the nonfibrillar state of both amyloid- $\beta$  and tau in Alzheimer's disease (AD). In this study, we used TR as a potential diagnostic marker of AD in frozen-thawed (F-T) brain tissue and imprint cytology. Control experiments included the use of Thioflavin-S staining, fixed tissue, and some double-labeled material with TR and selected tau markers, including AT100, MC1, Alz-50, TG-3, Tau-C3, and S396. Our results indicate that TR retains its strong affinity for both tangles and plaques in unfixed F-T tissue and imprint cytology. This information provides a potential use of TR as an accurate diagnostic tool for the rapid postmortem diagnosis of AD neuropathology. This study shows the advantages of TR on cytology mainly because tools for the fast postmortem diagnosis of AD are practically nonexistent. In addition, we observed Tau-C3 immunoreactivity in extracellular tangles, suggesting that the

Tau-C3 epitope is characteristically stable. Moreover, this study demonstrates that chemical fixation is not necessarily required for tau immunoreactivity on histological sections.

**Keywords** Touch imprint · Neuropathology · Thiazin red · Neurofibrillary tangle · Immunohistochemistry · Tau protein · Alzheimer's disease

## Introduction

Defining criteria for the postmortem diagnosis of Alzheimer's disease (AD) has proven to be difficult mainly caused by the phenotypical heterogeneity of the disease and the absence of a specific disease marker for AD. Even though the role played by amyloid- $\beta$  plaques and tangles in the pathogenesis of AD is not fully understood, a host of clinicopathological correlative studies have shown that both lesions, if present in a sufficient number, particularly in the neocortex, are still to be considered the best morphological hallmarks for the disease [1].

In general pathology, the use of cytology as a supplementary technique in autopsy diagnosis has found its way into the literature, but not into daily practice. Cytological techniques are reliable and technically simple. The sampling procedure is inexpensive because manpower and equipment needs are minimal. The staining and screening of slides can be done quickly during the autopsy so that the clinician can be furnished with a more accurate provisional diagnosis. This will potentially facilitate clinicopathological correlation and the rapid communication of information to the bereaved family [2]. Even though these are proved advantages of the cytological techniques for a fast neuropathological diagnosis, their use as a tool for the fast postmortem diagnosis of AD is practically nonexistent [3].

---

Jose Luna-Muñoz and Janneth Peralta-Ramirez contributed equally to this work.

---

J. Luna-Muñoz · R. Mena (✉)  
Departments of Physiology, Biophysics and Neurosciences,  
CINVESTAV-IPN, Mexico D.F., Mexico  
e-mail: rmena@fisio.cinvestav.mx

J. Peralta-Ramirez  
Department of Cell Biology, CINVESTAV-IPN,  
Mexico D.F., Mexico

L. Chávez-Macías  
Department of Pathology, Faculty of Medicine,  
General Hospital of Mexico, UNAM, Mexico City, Mexico

C. R. Harrington · C. M. Wischik  
Department of Mental Health,  
University of Aberdeen, Aberdeen, UK

Conventionally, the diagnostic confirmation of AD is evaluated by silver staining, which is the principal method of choice to detect  $\beta$ -amyloid plaques and neurofibrillary tangles (NFTs). Using this technique, it is also possible to label other pathological inclusions such as Pick bodies [4]. Though reactions in the silver solutions and those in the reducing agents are both difficult to standardize in the silver-staining method, it is sensitive, stable, and reproducible. The combination of immunohistochemistry with silver-staining methods has been extensively used in studies related to the analysis of  $\beta$ -amyloid deposits by using specific antigens. Although immunohistochemistry allows one to visualize a larger number of  $\beta$ -amyloid plaques than the silver-staining methods [5, 6], this is not so for tangles [7]. In addition, immunohistochemical detection is highly dependent on the antibody and experimental procedures such as the type of antibody and the proteolytic state of the tau molecule. These technical uncertainties make it difficult to use immunohistochemical detection as a standard for neuropathological diagnosis, especially when the quantity of deposits is of primary importance, as for the histological diagnostic criteria for AD [8, 9]. Both the methods require aldehyde fixation of the brain tissue. Despite these disadvantages some well-accepted criteria for the final diagnosis of AD include the use of immunohistochemical techniques [7].

The use of fresh tissue in a routine and systematic way can favor a precise and quick diagnosis in comparison to fixing either frozen or paraffin-embedded tissue. The cytology-imprint evaluation was developed by Duggeon and Patric in 1927 [10]. The cytology imprint in rapid diagnosis is used commonly by pathologists. However, the cytology imprint should preferably be used as a technique for immediate results and this analysis should be supplemented with later studies as silver staining and immunohistochemistry. In our laboratory, we routinely analyze brain tissue from AD cases obtained by autopsy. Characteristically, this tissue is paraformaldehyde-fixed before doing double and triple immunolabeling and confocal microscopy. Under these conditions, we have tested a variety of antibodies raised against normal and pathological species of the tau protein [11, 12]. In general, we include the use of the red fluorescent dye thiazin red (TR) as a counterstaining to be able to distinguish fibrillar from nonfibrillar states of tau aggregates [13, 14]. TR is excited at 540 nm and visualized in the red channel (580 nm). Our aim was to determine the diagnostic adequacy of touch-cytology imprints for identifying positive and negative NFTs and neuritic plaques in brains of AD cases with TR stain. Also, we wanted to investigate whether the absence of aldehyde fixation could affect the patterns of immunohistochemistry, at least for some selected tau markers. We also compared the TR technique with both Thioflavin-S and silver staining. The results

allow us to propose the use of TR as a tool for the fast and an accurate neuropathological diagnosis of AD in tissue imprints.

## Materials and methods

### Brain tissue

Brain tissue from six AD patients was examined in this study (age 47–90 years, mean 67.5 years, 2- to 6-h post-mortem delay). The diagnosis of AD was obtained by the NIA-NINCDS group criteria [15]. The clinical duration of the disease was from 5 to 15 years suggesting that they were severe with long-standing dementia.

### Touch imprint using TR

In this study based on the touch-imprint technique, all AD brain tissue was used frozen-thawed (F-T) (unfixed). The procedure for touch imprints was as follows. For each case, a block of approximately 0.5 cm<sup>3</sup> of F-T temporal cortex was immersed in a solution of the dye TR (0.001%) in water for 15 min at room temperature in the dark [16]. A direct imprint was then obtained by placing the unwashed block of tissue onto a glass slide and it was gently squeezed using a glass cover slip. Before coverslipping, the anti-queching medium Vectashield (Vector Labs., Burlingame) was added.

### Immunohistochemistry using the F-T AD brain tissue and TR counterstaining in touch imprints

Immunohistochemistry was done on the F-T tissue using antibodies raised to different tau protein epitopes (Table 1) and counterstaining with TR. The general characteristics of the set of antibodies used are listed in Table 1. F-T blocks from AD temporal cortical area (size of 0.5 cm<sup>3</sup>) were blocked with a solution of 0.2% IgG-free albumin (Sigma Chemical Co., St. Louis, MO) in PBS for 20 min at room temperature. Immunolabeled blocks were then incubated with the primary antibody TG-3 (IgM 1:40 dilution), Alz-50 (IgM 1:500 dilution), AT100 (IgG 1:500 dilution), Tau-C3 (IgG 1:500 dilution), or S396 (IgG 1:1,000 dilution) for 2 h at room temperature and then with FITC-tagged goat-anti-mouse IgM (or IgG) secondary antibody (Jackson Immuno. Res. Lab. Inc. West Grove). A PBS-0.2% Triton X-100 (Sigma Chemical Co., St. Louis, MO) solution was used in all the immunolabeling steps. The samples were counterstained with the dye TR to differentiate the nonfibrillar from fibrillar states of the tau aggregates [13, 14]. The antibody S396 has been used to detect late stages of tau processing in overt tangles [17–21]. After TR

**Table 1** Antibodies and recognition sites

Antibodies	Epitope	Isotype	Reference	
Alz-50, MC1	aa: 5–15, 312–322. Structural conformational change	Mo IgM, Mo IgG	[28–30]	
TG-3	aa: phospho Thr231. Regional conformational change	Mo IgM	[31]	
AT100	aa: phospho Ser199, Ser202, Thr205, Thr212, Ser214. Regional conformational change	Mo IgG	[32]	
<i>aa</i> amino acids, <i>Mo</i> Mouse, <i>Rb</i> Rabbit, <i>IgG</i> Immunoglobulin G, <i>IgM</i> Immunoglobulin M	Tau-C3	aa: Asp421 truncation	Mo IgG	[33]
	S396	aa: phospho Ser-396	Rb IgG	[34, 35]

counterstaining, touch imprints were obtained by placing the immunolabeled block tissue onto a glass slide and this was gently squeezed using a glass cover slip. The anti-quenching medium Vectashield (Vector Labs.) was also added.

#### Immunohistochemistry in paraformaldehyde-fixed brain tissue

To test the potential effects of aldehyde fixation on our results using touch imprints, we did immunohistochemistry on the fixed tissue. Selected blocks of temporal isocortex (size 0.5 cm<sup>3</sup>) of each AD brain tissue were fixed by immersion in a solution of 4% paraformaldehyde in PBS buffer, pH 7.4, at 4°C, for 30 min. After fixation, 50- $\mu$ m thick sections were obtained using a sliding microtome [13]. Immunolabeling was made following the conventional methodology that has been previously described [12]. Before coverslipping, the immunolabeled tissue was TR counterstained.

#### TR and Thioflavin-S staining in touch imprints

The human brain shows considerable autofluorescence in FITC and TRITC channels because of the abundance of highly fluorescent lipofuscin granules. Therefore, to avoid this inconvenience, before making the touch imprints in F-T brain tissue, a quenching procedure was used [22]. Briefly, brain blocks were incubated in 0.3% KMnO<sub>4</sub> for 3–5 min, then washed with water, and treated with a solution of 1% K<sub>2</sub>S<sub>2</sub>O<sub>5</sub> and 1% oxalic acid until the brown color was removed from the tissue (20–40 s). After a second wash with water, 1% sodium borohydride (NaBH<sub>4</sub>), which was prepared 2-h before use, was used for 5 min. The sample was then washed three times with distilled water and returned to PBS. Following method described in a previous report [22], samples were then stained with 0.05% Thioflavin-S in 50% ethanol in the dark for 8 min. This was followed by differentiation in two changes of 80% ethanol for 10-s each and three washes in large volumes of distilled water. Before the touch imprints, the brain tissue samples were incubated with TR (0.001% in water) for 15 min at room temperature in the dark. Touch imprints were obtained by placing the double-stained

block tissue onto a glass slide and it was gently squeezed using a glass cover slip. The anti-quenching medium Vectashield (Vector Labs.) was also added. As a control experimental, double staining with Thioflavin-S and TR, we followed similar procedures, as described above, using 50- $\mu$ m thick sections from paraformaldehyde-fixed brain blocks. Likewise, selected brain slices were stained using the Bielschowsky technique following a well-defined protocol [4, 23, 24].

#### Confocal microscopy

Double-immunolabeled sections were examined through a confocal laser scanning microscope (TCP-SP2, Leica, Heidelberg) using a 100 $\times$  oil-immersion Plan Apochromat objective (NA 1.4). Ten to 15 consecutive single sections were obtained at 0.8- to 1.0- $\mu$ m intervals for a sequential scan using two channels through the *z*-axis of the sample. The resulting stack of images was projected onto the two-dimensional plane using a pseudocolor display of green (FITC) and red (TRITC) and analyzed. Fluorochromes in double-labeled samples were excited at 488 nm (for FITC) and 568 nm (for TR). The resulting images were saved on compact disks.

#### Characteristics of Thiazin-red dye

We include a brief description of the characteristics of TR to better understand its properties as an accurate marker for the fast diagnosis of AD, as demonstrated in this paper. TR is an analog of naphthol-based azo structures whose functional characteristic is to bind  $\beta$ -pleated sheet structures, while providing a site to complex ferrous ion [16]. The affinity of TR for these type of structures was demonstrated by incubation with silk from *Bombyx mori* cocoons [16]. The red fluorescent dye TR was used for the first time in the staining of plaques and tangles in AD brains in 1988. Since 1995, TR has been extensively used in our laboratory in confocal microscopy-based studies on AD brains [12, 14, 25]. Recently, we studied double- and triple-immunolabeled brain tissues with a variety of abnormal tau epitopes, either hyperphosphorylated or truncated, combined with TR. These studies provided evidence that the use of TR is a

good strategy for modeling the earliest stages of tau processing leading to PHF formation in AD [12, 25]. TR fluorescence is excited in the range of 530–560 nm, monitoring red light emission above 580 nm [16].

## Results

NFT and amyloid plaque staining with TR, Thioflavin-S, and Bielschowsky silver techniques in paraformaldehyde-fixed AD brain tissue

Conventionally, AD neuropathological diagnosis is made in fixed brain tissue following well-known techniques including silver impregnations and, less frequently, the fluorescent dyes Congo red and Thioflavin-S [26]. As Fig. 1 shows, TR detects similar pathological structures, tangles (b, red channel), and plaques (e) as both Thioflavin-S (green channel, a, d) and the Bielschowsky silver-impregnation material (c, f).

### Thioflavin-S and TR staining in touch imprints

Contrasting with that observed in fixed tissue where Thioflavin-S clearly stained tangles, as Fig. 2 shows, in the F-T AD-tissue imprint this dye failed to detect the tangle (a, green channel) that is clearly detected by TR in the red channel (c). Similar results were obtained in a neuritic plaque detected by TR (d), but Thioflavin-S was unable to stain these structures (b).

Double labeling with conformational monoclonal antibodies (mAbs) MC1, Alz-50, AT100, TG-3, and 396 and TR in F-T AD brain-tissue touch imprints

To investigate whether the immunoreactivity of some conformational antibodies raised against either phosphodependent or truncated tau-related epitopes could be affected by the lack of fixation of the brain tissue, we tested patterns of immunoreactivity of primary antibodies MC1, Alz-50, AT100, TG-3, and S396 using confocal microscopy immunohistochemistry in F-T tissue touch imprints and counterstained with TR. As Fig. 3 shows, all the tested tau antibodies preserved their immunoreactivities in intracellular tangles (I-NFTs a–e, green channel). No evidence of immunolabeling of extracellular tangles (E-NFTs) was ever observed with the phosphodependent tau epitopes located along the N-terminus of tau (Fig. 3a–d). However, the antibody S396, which identifies a site of phosphorylation located at the C-terminus of the molecule clearly detected ghost tangles (Fig. 3e).

### Double labeling with mAbs Tau-C3 and TR in touch imprints in AD brains

We have recently demonstrated that the truncation at Asp-421, as detected by mAb Tau-C3, in addition to labeling I-NFTs, is already present in neuronal cells in a pretangle stage [25]. In conventional immunohistochemical procedures including fixed tissue, when we did mAb Tau-C3 immunolabeling and TR counterstaining, we observed

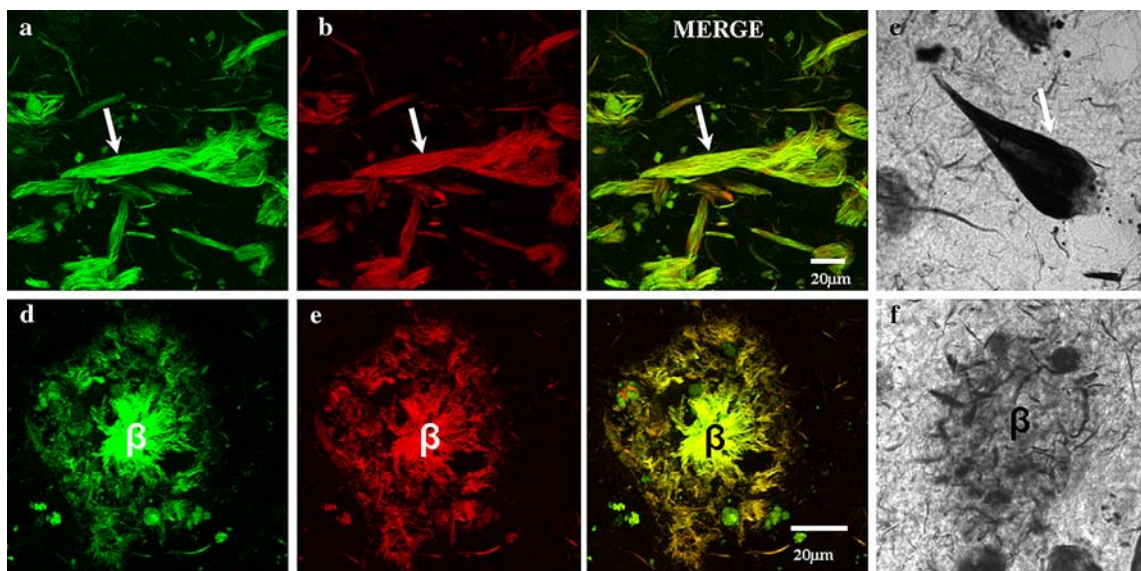
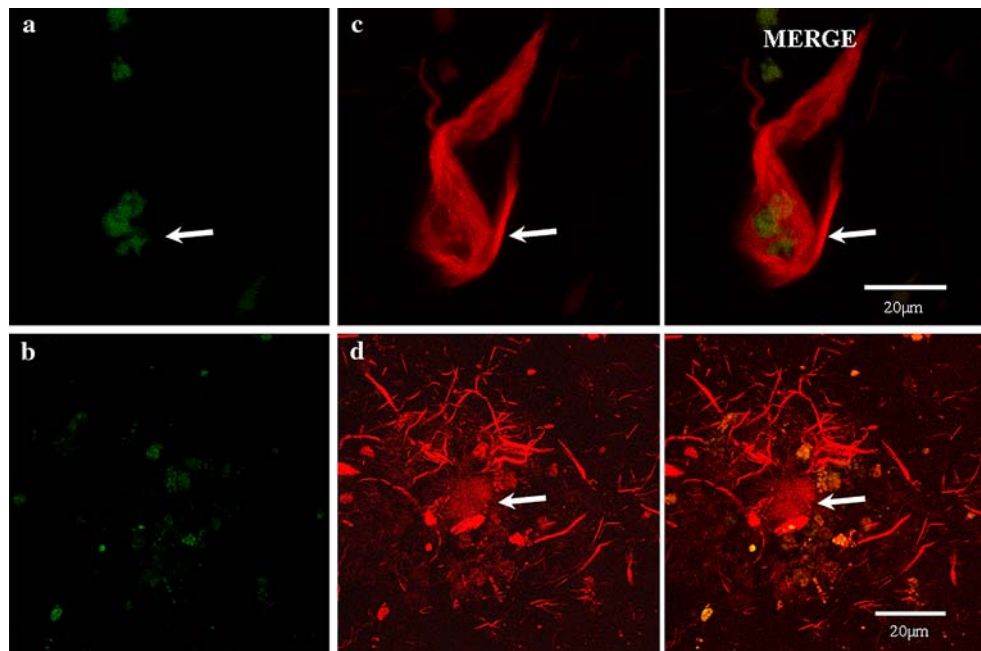


**Fig. 1** Fixed brain tissue sections from an AD case stained with silver impregnation (c, f) and double-stained with Thioflavin-S (a, d) and thiazin red (b, e). The three different stain techniques are able to detect

tangles (arrows in a–c) and neuritic plaques (d–f). The amyloid core is strongly detected by the two fluorescent dyes ( $\beta$  in d, e). Confocal microscopy



**Fig. 2** Touch imprints of AD-brain tissue blocks were double-stained with fluorescent dyes Thioflavin-S (**a, b green channel**) and thiazin red (**c, d red channel**). The dye thioflavin-S is unable to detect the tangle (**a**) and the neuritic plaque (**b**) that are clearly stained by TR in the red channel (**c, d**). Amyloid core (**arrow**). Confocal microscopy



similar patterns of staining as those well-described in aldehyde-fixed brain tissue [19, 25]. When we did mAb Tau-C3 and TR counterstaining in F-T tissue and touch imprints, as Fig. 4 shows, mAb Tau-C3 immunoreactivity was observed also in intracellular tangles (a) and the neuritic components of the amyloid plaque (c). However, mAb Tau-C3 immunoreactive deposits were also clearly observed in extracellular NFTs (Fig. 4b, large arrow) in touch imprints. These structures, which presumably may represent a subtype of ghost tangles, were partially detected by TR in the red channel (Fig. 4b, large arrow) but colocalized with mAb Tau-C3 immunolabeling. Another subtype of E-NFTs was detected by TR but undetected with mAb Tau-C3 (Fig. 4b, short arrow).

To test the potential effects of aldehyde fixation on our results using mAb Tau-C3 in E-NFTs, we performed double mAbs Tau-C3 and S396 immunolabeling on paraformaldehyde-fixed AD brain tissue. Our results indicate that mAb Tau-C3 immunoreactivity was occasionally observed in some E-NFTs, which were also identified by mAb S396 (Fig. 5, large arrow). In these cases, mAb Tau-C3 immunoreactivity displayed a weak pattern. The mAb Tau-C3 also identified some neurites located in the vicinity of the ghost tangle as well as some structures of amorphous profile that may represent lipofuscin granules. None of these structures were identified by mAb S396 in the red channel.

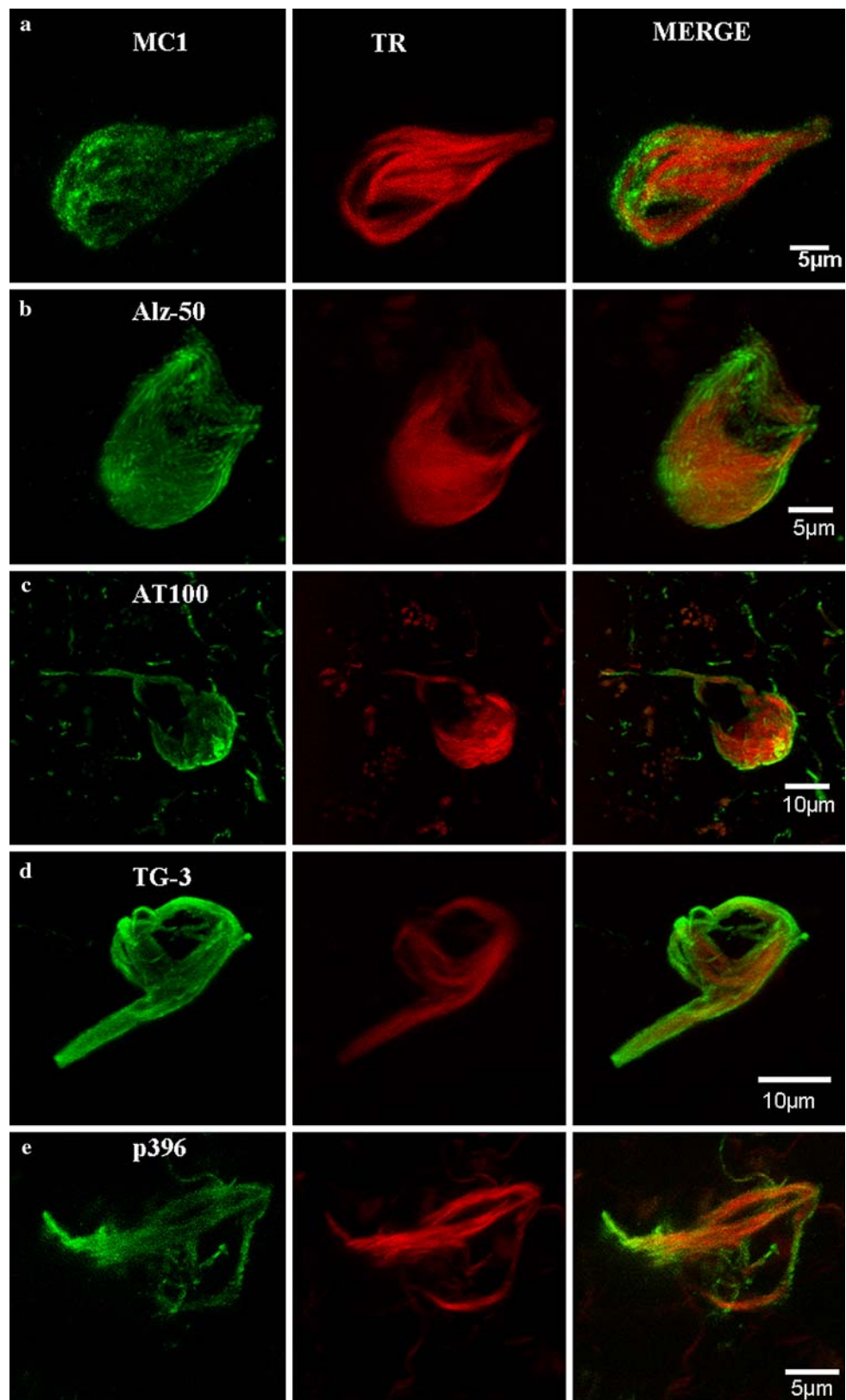
## Discussion

We have previously demonstrated in formalin-fixed AD brain tissue, that TR can be used like Thioflavin-S to detect

plaques and tangles [13]. This is also illustrated in this study (Fig. 1). In addition, we have also demonstrated because of its high affinity to  $\beta$ -pleated sheet conformations, that TR when combined with tau-related antibodies and the use of confocal microscopy is an accurate dye to differentiate fibrillar (assembled tau protein into PHF) from nonfibrillar (tau aggregates) states of the molecule [13, 14]. Moreover, in two recent reports by the use of combinations of antibodies raised against different phosphodependent tau epitopes with TR, we have demonstrated not only that abnormal phosphorylation of the *N*-terminus of the tau molecule in a soluble state precedes the conformational changes identified in an assembled PHF [12], but that the earliest stages of tau processing before their assembly into a PHF is characterized by the appearance of a specific cascade of events including phosphorylation and truncation [25]. In the present study, we now introduce evidence that TR preserves the same properties when used in F-T brain tissue from AD cases in touch imprints (Fig. 2). Thioflavin-S, a dye chemically similar to TR, does not preserve its affinity of plaques and tangles in F-T AD brain tissue (Fig. 2). This finding per se provides more advantages of TR over Thioflavin-S. Touch imprint procedures have been made in the AD brain but using the dye Congo red, which provides a characteristic birefringence staining [3]. However TR, as a red fluorescent marker whose properties permit its combination with any tau marker in both the green (FITC) and/or the blue channel (Cy5), is also useful for studies related to mechanisms of tau processing in AD [12, 13, 25].

Because TR is useful for both immunohistochemistry confocal studies and in F-T AD-brain tissue staining, in this

**Fig. 3** Touch imprints of AD tissue blocks were immunolabeled with antibodies MC1 (a), Alz-50 (b), AT100 (c), TG-3 (d), and 396 (e). TR counterstaining (red channel). This set of antibodies was raised against different epitopes in PHF-tau (Table 1). All the phosphodependent (TG-3 and AT100) and conformational (Alz-50 and MC1) antibodies identified intracellular NFTs that are also detected by TR in the red channel. The tangle in (e) is strongly immunolabeled with both mAb S396 and TR. Confocal microscopy



study we performed double and triple immunolabeling and confocal microscopy following similar protocols as those previously described [11, 12, 18, 19, 25]. Our findings

demonstrated that in touch imprints tau-PHF-related epitopes (Table 1) are able to bind specific antibodies. Therefore, the chemical fixation is not required for tau

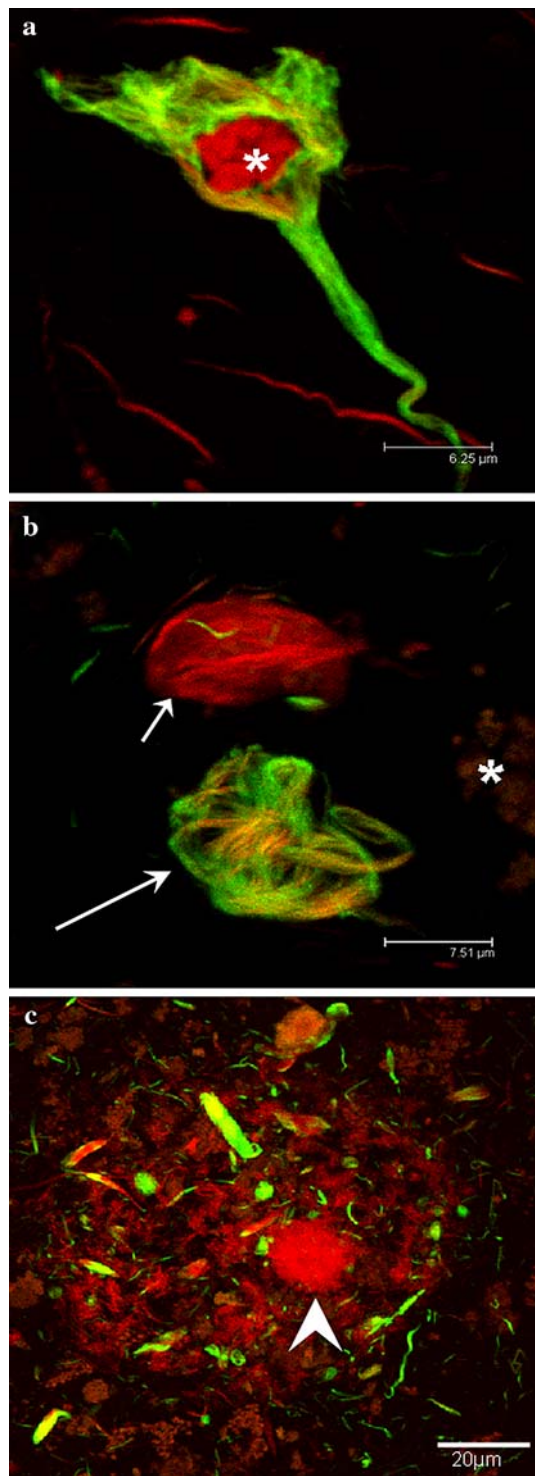


**Fig. 4** mAb Tau-C3 immunolabeling (*green channel*) in touch imprints AD-brain tissue blocks and TR counterstained (*red channel*). mAb Tau-C3 detected both intracellular (**a**) and extracellular (**b**) tangles. TR partially detected both types of such structures. However, TR was able to detect a subtype of an extracellular structure (*arrows in b, red channel*) located in the vicinity that was not identified by mAb Tau-C3. Likewise, mAb Tau-C3 also detected the majority of the neuritic component of the amyloid plaque. TR clearly detected the amyloid core in the *red channel* (*arrowhead in c*). Confocal microscopy

immunoreactivity because tau epitopes in this F-T tissue are closer to the extracted tau molecules used to make biochemical assays. By proving that tau immunoreactivity is preserved in F-T tissue, it is possible to make better correlations between morphological and biochemical observations. In addition, once we proved that the patterns of tau immunoreactivity in both fixed and F-T AD-brain tissue are much alike, we can assume that at least those models explaining steps of the molecular mechanisms involved in tau phosphorylation processing, which have been based upon the used of aldehyde-fixed tissue and immunohistochemistry, reflect the actual nature of the molecular events occurring in AD neuropathology.

In contrast to that observed in aldehyde-fixed tissue, for touch imprints of F-T AD-brain tissue, mAb Tau-C3 is able to detect not only intracellular tangles but extracellular or “ghost” structures. This finding is in disagreement with previous reports that have supported the belief that mAb Tau-C3 immunoreactivity is restricted to I-NFTs [19, 20, 27]. Freezing, type of aldehyde, fixation time, and postmortem delay may be some factors that explain the different patterns of immunolabeling of truncated tau-related mAb Tau-C3 in NFTs. We can speculate, as a consequence of crystal formation caused by fast freezing, that this may somewhat cause the breaking of the neuronal plasma membrane thus exposing the intracellular PHF bundles to the extracellular space to become extracellular structures. However, the differential pattern of Tau-C3 immunolabeling in tangles was not observed in any of the other tau-related antibodies included in this study (AT100, TG-3, MC1, Alz-50). Thus, mAb Tau-C3 immunoreactivity in E-NFTs may be specifically related to the molecular mechanisms of tau processing, involving endogenous proteolysis at Asp-421, which because of the aldehyde fixation may somehow become occluded and therefore undetected by mAb Tau-C3. From this, the proposed sequences of tau processing as described by the use of specific tau-related markers [19, 20, 27] may be important to be reevaluated. More detailed analysis is required to support this suggestion. Because all the brain specimens that were available to this study were fast-frozen, we were unable to test whether cryprotection pretreatment of the tissue before freezing may also unmask Tau-C3 immunoreactivity in extracellular NFTs.

We can conclude that the intensity of TR staining and the simplicity and reproducibility of the short time of the touch imprint using TR suggest that it may be a useful complementary tool to the standard techniques used for the evaluation of AD neuropathology. In addition, this technique may be potentially useful to make a diagnosis of AD during autopsy so that fixed brain tissue is no longer required. This may be particularly interesting for those countries where removing the brain and burying the body



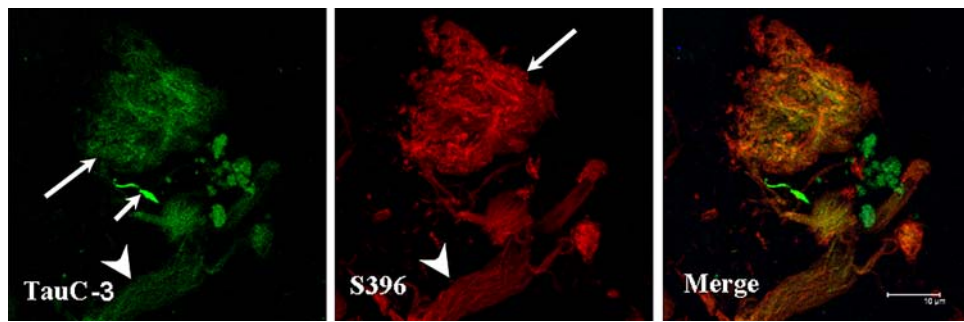


**Fig. 5** Fixed AD brain sections were double immunolabeled with antibodies Tau-C3 and S396. A portion of the extracellular tangle (*arrow*) strongly detected by the antibody S396 (*red channel*) is identified by Tau-C3 in the *green channel*. Likewise, a very weak

immunolabeling is observed with Tau C3 in the enlarged neurite located at the bottom of the figure (*arrowhead, red channel*). However, a cluster of dystrophic neurites are detected only by Tau-C3 (*small arrows*)

without the brain poses a major ethical issue to the public or introduces legal problems.

**Acknowledgments** Authors want to express their gratitude to Dr. P. Davies (Albert Einstein College of Medicine, Bronx, NY, USA) for the generous gift of mAbs TG-3, Alz-50 and MC1. Dr. L. Binder is kindly acknowledged for the donation of mAb Tau-C3. also Mr. José L. Fernández for the handling of the human brain tissue, and Ms. Maricarmen De Lorenz for her secretarial assistance. This work was financially supported by CONACyT grant, No. 47630 (to R.M.). Thanks to Dr. Ellis Glazier for editing the English-language text.

## References

- Jellinger KA, Bancher C (1997) Proposals for re-evaluation of current autopsy criteria for the diagnosis of Alzheimer's disease. *Neurobiol Aging* 18:S55–S65
- Dada MA, Ansari NA (1997) Post-mortem cytology: a reappraisal of a little used technique. *Cytopathology* 8:417–420
- McLean CA, Harney MC, Gonzales MF (1994) Cytological demonstration of features of Alzheimer's disease using brain smear technique. *Diagn Cytopathol* 10:320–325
- Uchihara T (2007) Silver diagnosis in neuropathology: principles, practice and revised interpretation. *Acta Neuropathol* 113:483–499
- Allsop D, Haga SI, Haga C, Ikeda SI, Mann DM, Ishii T (1989) Early senile plaques in Down's syndrome brains show a close relationship with cell bodies of neurons. *Neuropathol Appl Neurobiol* 15:531–542
- He Y, Duyckaerts C, Delaere P, Piette F, Hauw JJ (1993) Alzheimer's lesions labelled by anti-ubiquitin antibodies: comparison with other staining techniques. A study of 15 cases with graded intellectual status in ageing and Alzheimer's disease. *Neuropathol Appl Neurobiol* 19:364–371
- Braak Alafuzoff I, Arzberger T et al (2006) Staging of Alzheimer disease-associated neurofibrillary pathology using paraffin sections and immunocytochemistry. *Acta Neuropathol* 112:389–404
- Duyckaerts C, Delaere P, Hauw JJ, Abbamondi-Pinto AL, Sorbi S, Allen I, Brion JP, Flament-Durand J, Duchon L, Kauss J (1990) Rating of the lesions in senile dementia of the Alzheimer type: concordance between laboratories. A European multicenter study under the auspices of EURAGE. *J Neurol Sci* 97:295–323
- Mirra SS, Heyman A, McKeel D, Sumi SM, Crain BJ, Brownlee LM, Vogel FS, Hughes JP, van Belle G, Berg L (1991) The Consortium to establish a registry for Alzheimer's disease (CERAD). Part II. Standardization of the neuropathologic assessment of Alzheimer's disease. *Neurology* 41:479–486
- Suen KC, Wood WS, Syed AA, Quenville NF, Clement PB (1978) Role of imprint cytology in intraoperative diagnosis: value and limitations. *J Clin Pathol* 31:328–337
- Garcia-Sierra F, Hauw JJ, Duyckaerts C, Wischik CM, Luna-Munoz J, Mena R (2000) The extent of neurofibrillary pathology in perforant pathway neurons is the key determinant of dementia in the very old. *Acta Neuropathol* 100:29–35
- Luna-Munoz J, Garcia-Sierra F, Falcon V, Menendez I, Chavez-Macias L, Mena R (2005) Regional conformational change involving phosphorylation of tau protein at the Thr231, precedes the structural change detected by Alz-50 antibody in Alzheimer's disease. *J Alzheimers Dis* 8:29–41
- Mena R, Edwards P, Perez-Olvera O, Wischik CM (1995) Monitoring pathological assembly of tau and beta-amyloid proteins in Alzheimer's disease. *Acta Neuropathol* 89:50–56
- Mena R, Edwards PC, Harrington CR, Mukaetova-Ladinska EB, Wischik CM (1996) Staging the pathological assembly of truncated tau protein into paired helical filaments in Alzheimer's disease. *Acta Neuropathol* 91:633–641
- McKhann G, Drachman D, Folstein M, Katzman R, Price D, Stadlan EM (1984) Clinical diagnosis of Alzheimer's disease: report of the NINCDS-ADRDA Work Group under the auspices of Department of Health and Human Services Task Force on Alzheimer's Disease. *Neurology* 34:939–944
- Resch JF, Scott GL, Wischik CM (1991) Design and synthesis of a potential affinity/cleaving reagent for beta-pleated sheet protein structures. *Bioorg Med Chem Lett* 1:519–522
- Basurto-Islas G, Luna-Munoz J, Guillozet-Bongaarts AL, Binder LI, Mena R, Garcia-Sierra F (2008) Accumulation of aspartic acid421- and glutamic acid391-cleaved tau in neurofibrillary tangles correlates with progression in Alzheimer disease. *J Neuropathol Exp Neurol* 67:470–483
- Galvan M, David JP, Delacourte A, Luna J, Mena R (2001) Sequence of neurofibrillary changes in aging and Alzheimer's disease: A confocal study with phospho-tau antibody, AD2. *J Alzheimers Dis* 3:417–425
- Garcia-Sierra F, Ghoshal N, Quinn B, Berry RW, Binder LI (2003) Conformational changes and truncation of tau protein during tangle evolution in Alzheimer's disease. *J Alzheimers Dis* 5:65–77
- Guillozet-Bongaarts AL, Garcia-Sierra F, Reynolds MR, Horowitz PM, Fu Y, Wang T, Cahill ME, Bigio EH, Berry RW, Binder LI (2005) Tau truncation during neurofibrillary tangle evolution in Alzheimer's disease. *Neurobiol Aging* 26:1015–1022
- Mondragon-Rodriguez S, Basurto-Islas G, Santa-Maria I, Mena R, Binder LI, Avila J, Smith MA, Perry G, Garcia-Sierra F (2008)

- Cleavage and conformational changes of tau protein follow phosphorylation during Alzheimer's disease. *Int J Exp Pathol* 89:81–90
22. Sun A, Nguyen XV, Bing G (2002) Comparative analysis of an improved thioflavin-s stain, Gallyas silver stain, and immunohistochemistry for neurofibrillary tangle demonstration on the same sections. *J Histochem Cytochem* 50:463–472
  23. Uchiyama T, Nakamura A, Yamazaki M, Mori O (2001) Evolution from pretangle neurons to neurofibrillary tangles monitored by thiazin red combined with Gallyas method and double immunofluorescence. *Acta Neuropathol* 101:535–539
  24. Uchiyama T, Shibuya K, Nakamura A, Yagishita S (2005) Silver stains distinguish tau-positive structures in corticobasal degeneration/progressive supranuclear palsy and in Alzheimer's disease—comparison between Gallyas and Campbell-Switzer methods. *Acta Neuropathol* 109:299–305
  25. Luna-Munoz J, Chavez-Macias L, Garcia-Sierra F, Mena R (2007) Earliest stages of tau conformational changes are related to the appearance of a sequence of specific phospho-dependent tau epitopes in Alzheimer's disease. *J Alzheimers Dis* 12:365–375
  26. Styren SD, Hamilton RL, Styren GC, Klunk WE (2000) X-34, a fluorescent derivative of Congo red: a novel histochemical stain for Alzheimer's disease pathology. *J Histochem Cytochem* 48:1223–1232
  27. Binder LI, Guillozet-Bongaarts AL, Garcia-Sierra F, Berry RW (2005) Tau, tangles, and Alzheimer's disease. *Biochim Biophys Acta* 1739:216–223
  28. Carmel G, Mager EM, Binder LI, Kuret J (1996) The structural basis of monoclonal antibody Alz50's selectivity for Alzheimer's disease pathology. *J Biol Chem* 271:32789–32795
  29. Jicha GA, Bowser R, Kazam IG, Davies P (1997) Alz-50 and MC-1, a new monoclonal antibody raised to paired helical filaments, recognize conformational epitopes on recombinant tau. *J Neurosci Res* 48:128–132
  30. Wolozin B, Davie P (1987) Alzheimer-related neuronal protein A68: specificity and distribution. *Ann Neurol* 22:521–526
  31. Jicha GA, Lane E, Vincent I, Otvos L, Hoffmann R Jr, Davies P (1997) A conformation- and phosphorylation-dependent antibody recognizing the paired helical filaments of Alzheimer's disease. *J Neurochem* 69:2087–2095
  32. Zheng-Fischhofer Q, Biernat J, Mandelkow EM, Illenberger S, Godemann R, Mandelkow E (1998) Sequential phosphorylation of Tau by glycogen synthase kinase-3beta and protein kinase A at Thr212 and Ser214 generates the Alzheimer-specific epitope of antibody AT100 and requires a paired-helical-filament-like conformation. *Eur J Biochem* 252:542–552
  33. Gamblin TC, Chen F, Zambrano A, Abraha A, Lagalwar S, Guillozet AL, Lu M, Fu Y, Garcia-Sierra F, LaPointe N, Miller R, Berry RW, Binder LI, Cryns VL (2003) Caspase cleavage of tau: linking amyloid and neurofibrillary tangles in Alzheimer's disease. *Proc Natl Acad Sci U S A* 100:10032–10037
  34. Liu F, Iqbal K, Grundke-Iqbal I, Gong CX (2002) Involvement of aberrant glycosylation in phosphorylation of tau by cdk5 and GSK-3beta. *FEBS Lett* 530:209–214
  35. Liu F, Zaidi T, Iqbal K, Grundke-Iqbal I, Merkle RK, Gong CX (2002) Role of glycosylation in hyperphosphorylation of tau in Alzheimer's disease. *FEBS Lett* 512:101–106